Article

$M_xCo_3O_4$/g-C_3N_4 Derived from Bimetallic MOFs/g-C_3N_4 Composites for Styrene Epoxidation by Synergistic Photothermal Catalysis

REN Fengdi, GAO Qiqin* and CHEN Yuzhen✉

Received September 26, 2022
Accepted November 3, 2022

Although metal-organic frameworks(MOFs) have been widely reported as precursors for obtaining various porous materials in recent years, the limited MOF types and monofunctional active site of MOF-based catalysts remain to be hard to crack. Herein, bimetallic MOFs, MCo-ZIFs stabilized by graphitized carbon nitride(g-C_3N_4) and their pyrolytic $M_xCo_3O_4$/g-C_3N_4 hybrids(M=Zn, Cu, Fe, Ni) have been designedly synthesized. The obtained $M_xCo_3O_4$/g-C_3N_4 hybrids display synergistic photothermal effect from both $M_xCo_3O_4$ and g-C_3N_4 under visible light irradiation. Significantly, the solution temperature can be heated from room temperature(20 °C) to 66 °C after 40 min irradiation. Therefore, the catalytic activity of $M_xCo_3O_4$/g-C_3N_4 exceeds those of most reported catalysts under mild reaction conditions. The optimal $Zn_xCo_3O_4$/g-C_3N_4 catalyst realizes 96% conversion and 75% selectivity toward styrene oxide within 20 min. Incredibly, the $Cu_xCo_3O_4$/g-C_3N_4 could achieve up to 89% selectivity toward styrene oxide. To our knowledge, this is the first report about the novel photothermal effect of ZIFs-derived metal oxides.

Keywords Metal-organic framework; Pyrolysis; Photothermal effect; Styrene epoxidation

1 Introduction

Styrene epoxide(SO) is an important intermediate for the synthesis of epoxy diluent, pharmaceutical, and most fine chemicals in chemical industry[1]. The reaction of styrene epoxidation to produce SO has always received much attention[2]. Practically, the oxidizing agents for styrene epoxidation are mainly peroxic acid or chloropropane[3], which readily produce by-product and may bring serious environmental pollution. In addition, to achieve high selectivity toward oxidized styrene, prooxygenic agent, such as H_2O_2, *tert*-butyl hydroperoxid(TBHP) or peracids, high temperature, high pressure and/or noble metal-based catalysts are usually required[4−6]. However, these harsh reaction conditions are disadvantagous to the recyclability and useful long-life of metal catalysts.

The noble metal catalysts, such as Au and Ag-based catalysts have shown wonderful catalytic activity in the epoxidation of styrene[7−9]. However, obtaining pure SO or high selectivity remains to be a great challenge under moderate reaction conditions. Therefore, it is necessary to develop novel, low cost and effective metal catalysts to achieve high SO selectivity at room temperature.

As one of new crystalline porous materials, metal-organic frameworks(MOFs) are composed of organic ligands and transitional metal ions or MO_x[10−15]. Benefitting from the well-ordered porosity and large surface areas, tunable pore size and morphology, MOFs have been extensively applied in heterogeneous catalysis[16−19], gas storage[20] and separation[21,22], sensors[23], and so on. Furthermore, MOFs have been deemed as excellent templates or precursors to obtain various porous carbon-based composites[24−29]. These hybrids have higher chemical/thermal stabilities, more abundant active sites, as well as good electrical conductivity compared with their parent MOFs[30−34]. Especially in recent years, the pyrolysis of MOFs develops very rapidly and a large number of related references emerge in endlessly[35−44]. As a classical MOF, zeolitic imidazolate framework(ZIF) has received tremendous popularity due to its facile synthesis, abundant N contents and flexibly doped active transitional metals(*e.g.*, Cu/Co/Ni)[45]. Therefore, ZIFs-derived metal/carbon catalysts or metal oxides have received widespread attentions in electrocatalysis[46−49], heterogeneous catalysis[50−52] and photocatalysis fields[53−57]. However, although ZIFs have be assembled with various materials, the multifunctionality of their derivatives is still difficult to be realized.

Graphitized carbon nitride(g-C_3N_4) has attracted strong attentions due to its unique layered structure, high chemical-stability, photosensitive property and low-cost[58−64]. At present, g-C_3N_4 exhibits potential application prospects in many fields, such as photocatalysis[65,66], electrocatalysis[67,68] and energy storage[69]. The g-C_3N_4 has proved to be an ideal carrier because it not only could stabilize and disperse the active species, but also promotes the electron transfer among them[70,71].

In this work, we successfully immobilized bimetallic ZIFs on g-C_3N_4 as precusors by simple assembly. Their pyrolytic $M_xCo_3O_4$/g-C_3N_4 hybrids possess high selectivity and conversion toward SO in styrene epoxidation reaction under

✉ CHEN Yuzhen
chenzhen1738@163.com
*This author is working in Dongming Country Second Junior Middle School, Heze 274500, P. R. China.
Department of Chemistry, College of Chemistry and Chemical Engineering, Qingdao University, Qingdao 266071, P. R. China

https://doi.org/10.1007/s40242-022-2292-6

visible light irradiation. The superior catalytic performance mainly comes from the synergistic photothermal effect between $M_xCo_3O_4$ and g-C_3N_4, which greatly raises the solution temperature from 20 °C to 66 °C. Furthermore, bimetallic active Cu and Co sites ensure both good activity and high selectivity. g-C_3N_4 effectively disperses metal particles and thus exposes more catalytic active sites. This research firstly discovered the photothermal effects of ZIF-derived oxides, which would open a door to a new world about MOFs.

2 Experimental

2.1 Materials and Characterization

All chemicals are from commercial sources and used without further purification: acetonitrile(C_2H_3N, A. R.), methanol (CH_3OH, A. R.), styrene(C_8H_8, A. R), isobutyraldehyde(C_4H_8O, A. R.), copper nitrate trihydrate[$Cu(NO_3)_2·3H_2O$, A. R.], zinc nitrate hexahydrate[$Zn(NO_3)_2·6H_2O$, A. R.], cobalt nitrate hexahydrate[$Co(NO_3)_2·6H_2O$, A. R.], 2-methylimidazole ($C_4H_6N_2$, A. R.), nickel nitrate hexahydrate[$Ni(NO_3)_2·6H_2O$, A. R.], and lauryl sodium sulfate($C_{12}H_{25}SO_4Na$, A. R.) were purchased from Sinopharm Chemical Reagent Co., Ltd.

Power X-ray diffraction(PXRD) patterns were carried out on a Rigaku Saturn 70 diffractometer at 113 K with Mo$K\alpha$ radiation (λ=0.071073 nm). Nitrogen sorption measurement was conducted using a Micromeritics ASAP 2020 system at 77 K. Scanning electron microscopy(SEM) images were acquired on a JEOL JSM-7800F at an acceleration voltage of 10 kV. The transmission electron microscopy(TEM) image, were obtained on a Tecnai G2 20 with an electron acceleration energy of 200 kV. The contents of mentals in samples were analyzed by an Agilent ICP-OES 730 inductively coupled plasma atomic emission spectrometer(ICP-AES). Catalytic reaction products were analyzed and identified by means of gas chromatography (GC, Shimadzu 2030 Plus). The UV-Vis diffuse reflectance spectroscopy(DRS) spectra of catalysts were measured using $BaSO_4$ as a reference on a PerkinElmer Lamda-950 spectrophotometer.

2.2 Preparation and Characterization of Catalysts

2.2.1 Synthesis of g-C_3N_4 and Surface Treatment

The synthesis method of g-C_3N_4 was mainly adopted from previous literature[72,73]. Briefly, 5 g of urea was calcined at 500 °C for 3 h at a heating rate of 5 °C/min under N_2 atmosphere. Finally, some light yellow powders were collected. For treatment, 50 mg of lauryl sodium sulfate was dissolved in 10 mL of ultrapure water, after which 150 mg of g-C_3N_4 and 10 mL of methanol were added. The mixture was dispersed by ultrasound for 5 h and then centrifuged with methanol three times and dried at room temperature. Finally, it was stored in an air-tight container for further use.

2.2.2 Synthesis of ZIF-67 and MCo-ZIFs

The synthesis of ZIF-67 was mainly based on a previous procedure with simple modifications[74]. $Co(NO)_3·6H_2O$ (6 mmol) was dispersed in 20 mL of deionized water to attain solution a. And 0.27 mol of 2-methylimidazole was dispersed in 100 mL of deionized water to attain solution b. Then solution b was added to solution a, and stired at room temperature for 6 h. The obtained sample was dried in a vacuum oven for 12 h at 60 °C for further use. The MCo-ZIF synthetic process was the same to that of ZIF-67, except by changing the solution volume of metallic precursors(the total mole of M^{2+} and Co^{2+} is 6 mmol, M=Zn, Cu, Ni, Fe).

2.2.3 Synthesis of ZIF-67/g-C_3N_4 and MCo-ZIF/g-C_3N_4

First, g-C_3N_4(1 g) was dissolved in 50 mL of deionized water, and dispersed by ultrasound for 30 min to obtain solution A. $Co(NO)_3·6H_2O$(6 mmol) was dissloved in 20 mL of deionized water, followed by an ultrasonic treatment for 30 min to obtain solution B. 2-Methylimidazole(0.27 mol) was dissolved in 100 mL of deionized water to obtain solution C. Then solution C was added to solution B dropwise under vigorous stirring. The resulting mixture was stired at room temperature for 6 h, and dried in a vacuum oven for 12 h at 60 °C for further use. The synthetic process of MCo-ZIF/g-C_3N_4 was the same to that of ZIF-67, except by changing the solution volume of metallic precursors(the total mole of M^{2+} and Co^{2+} is 6 mmol, M=Zn, Cu, Ni, Fe).

2.2.4 Synthesis of Co_3O_4/g-C_3N_4 and $M_xCo_3O_4$/g-C_3N_4

The above composites were calcined at 400 °C for 2 h at a heating rate of 5 °C/min under air atmosphere to finally attain Co_3O_4/g-C_3N_4 and $M_xCo_3O_4$/g-C_3N_4. For comparison, Co_3O_4 and $M_xCo_3O_4$ were also synthesized through a similar pyrolysis procedure.

2.3 Styrene Epoxidation

Catalyst(30 mg) was dispersed into 20 mL of acetonitrile, and then 0.1 mmol of styrene and 2 mmol of isobutyraldehyde were added to the suspensions. The mixture was bubbling with oxygen under visible-light irradiation($\lambda \geqslant 420$ nm) for reaction. During the reaction process, the solution was regularly monitored by GC.

https://doi.org/10.1007/s40242-022-2292-6

3 Results and Discussion

Fig.1 illustrates the *in-situ* growth of MCo-ZIF on g-C_3N_4 surface and the subsequent heat treatment at air atmosphere for obtaining bimetallic oxide/g-C_3N_4(denoted as $M_xCo_3O_4$/g-C_3N_4). The composites perform synergistic photothermal effect and excellent catalytic performance toward the reaction of styrene epoxidation under visible light irradiation.

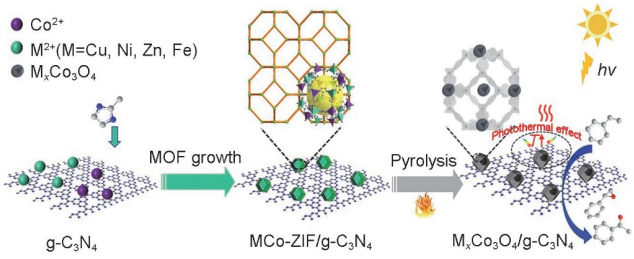

Fig.1 Schematic illustration for the preparation of $M_xCo_3O_4$/g-C_3N_4 and their synergistic catalysis

3.1 Structure Characterization

The crystal structures of MCo-ZIFs and MCo-ZIFs/g-C_3N_4 were characterized and analyzed by powder X-ray diffraction (PXRD). As shown in Fig.2(A), all the as-synthesized MCo-ZIFs have identical diffraction peaks as the simulated ZIF-67, indicating the bimetallic ZIFs were successfully synthesized. For MCo-ZIF/g-C_3N_4, except for the typical diffraction peaks of ZIF, two characteristic peaks at 2θ=13.1°(100) and 27.4°(002) belong to g-C_3N_4. PXRD patterns of $Zn_xCo_3O_4$ and $Cu_xCo_3O_4$

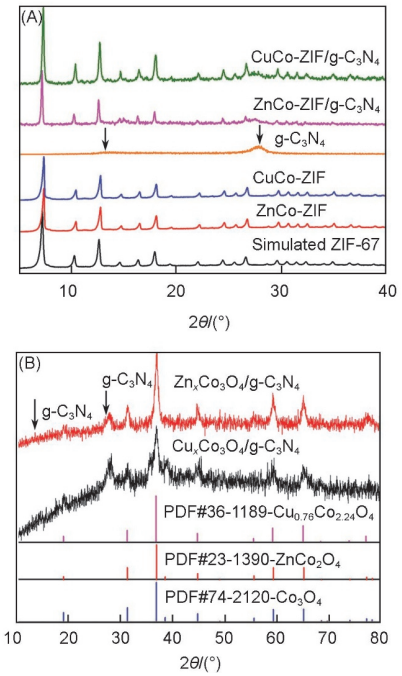

Fig.2 PXRD patterns of simulated ZIF-67, as-synthesized ZnCo-ZIF, CuCo-ZIF, g-C_3N_4, ZnCo-ZIF/g-C_3N_4 and CuCo-ZIF/g-C_3N_4(A), and $Zn_xCo_3O_4$/g-C_3N_4 and $CuxCo_3O_4$/g-C_3N_4(B)

stabilized by g-C_3N_4 as shown in Fig.2(B) suggested their successful assembly.

The Cu and Co contents in $M_xCo_3O_4$ with different Cu/Co molar proportions were measured by inductively coupled plasma atomic emission spectroscopy(ICP-AES)(Table S1, see the Electronic Supplementary Material of this paper). Combining the diffraction data of metal oxides and the actual metal contents of Co, Zn and Cu, it is not hard to infer the specific compositions of $Zn_xCo_3O_4$ and $Cu_xCo_3O_4$ are $Cu_{0.76}Co_{2.24}O_4$/Co_3O_4 and $ZnCo_2O_4$/Co_3O_4, respectively. These results further demonstrate that $M_xCo_3O_4$ were successfully immobilized on g-C_3N_4. Among all the materials, ZnCo-ZIF/g-C_3N_4, Cu_2Co_1-ZIF/g-C_3N_4 and their derivates have been further investigated as representative.

The morphologies of ZnCo-ZIF/g-C_3N_4 and CuCo-ZIF/g-C_3N_4 were measured by SEM. Fig.3(A) and (B) show their regular dodecahedron morphology and the MOF particles are highly dispersed on g-C_3N_4. The TEM image of Fig.4(A) obviously indicates the layered structure in g-C_3N_4. The images of Fig.4(B) and (C) display the uniform dispersion of bimetallic ZIF particles(average size, 1 μm) on g-C_3N_4, which demonstrate their successful recombination. The images of Fig.4(D) and (E) show the successful formation of $M_xCo_3O_4$/g-C_3N_4 with retained sizes and morphology from their precursors. N_2 sorption experiments in Fig.4(F) reveal that the Brunauer-Emmett-Teller(BET) surface areas of ZnCo-ZIF/g-C_3N_4 and $Zn_xCo_3O_4$/g-C_3N_4 are 666 and 14 cm^2/g, respectively. The decreased surface areas after calcination are mainly due to the increased mass accompanied by the carbon loss and metal oxides formation. In addition, during calcination process, the inevitable structural collapse makes the pore structure in the $Zn_xCo_3O_4$/g-C_3N_4 change from micropore to mesoporous. However, the remained porous structure guarantees the good adsorption capacity of $M_xCo_3O_4$/g-C_3N_4 taword the oxygen molecules, and the sufficient contaction between the reaction substrates with the active sites(Fig.S1, see the Electronic Supplementary Material of this paper).

Light absorption performance is a crucial prerequisite for photocatalysts[75—78]. The UV-Vis diffuse reflectance spectra are investigated to determine the light-absorption ability of the samples in Fig.5(A). Pure g-C_3N_4 has a visible light absorption band at 330—450 nm. The stronger light response signal of Co_3O_4/g-C_3N_4 and $Zn_xCo_3O_4$/g-C_3N_4 than those of Co_3O_4 and $Zn_xCo_3O_4$ in the range of 350—450 nm indicates their synergetic photothermal properties. Fig.5(B) reflects the variations of solution temperature in the presence of different catalysts along with the irradiation time. The results indicate that all samples have different photothermal conversion efficiencies under xenon lam irradiation($\lambda \geqslant 420$ nm). Compared to commercial Co_3O_4, the Co-ZIF derived porous Co_3O_4 performs better maximum thermal conversion and increases the solution

https://doi.org/10.1007/s40242-022-2292-6

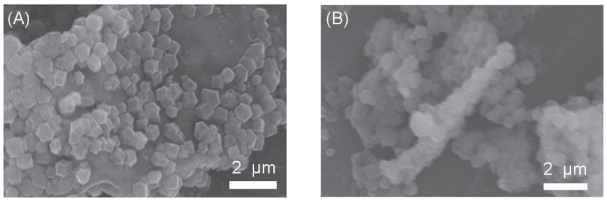

Fig.3 SEM images of ZnCo-ZIF/g-C_3N_4(A) and CuCo-ZIF/g-C_3N_4(B)

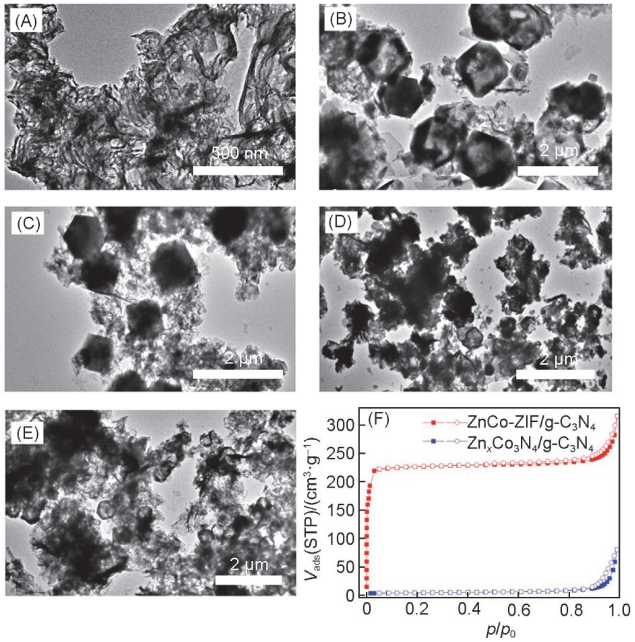

Fig.4 TEM images of g-C_3N_4(A), ZnCo-ZIF/g-C_3N_4(B), CuCo-ZIF/g-C_3N_4(C), $Zn_xCo_3O_4$/g-C_3N_4(D), and $Cu_xCo_3O_4$/g-C_3N_4(E) and N_2 sorption isotherms of ZnCo-ZIF/g-C_3N_4 and $Zn_xCo_3O_4$/g-C_3N_4 at 77 K(F)

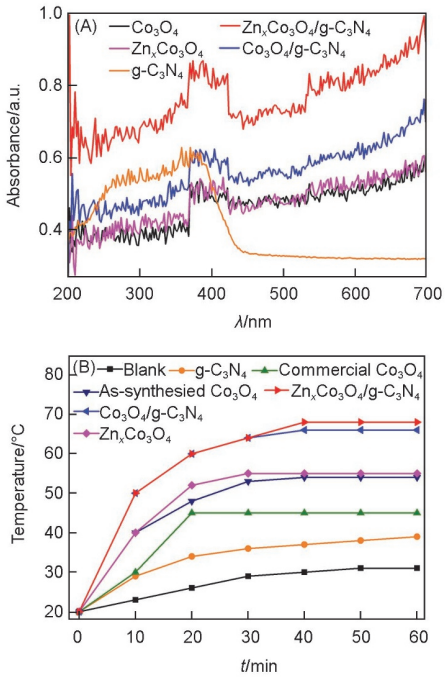

Fig.5 UV-Vis absorption spectra for $Zn_xCo_3O_4$/g-C_3N_4, Co_3O_4/g-C_3N_4, $Zn_xCo_3O_4$, Co_3O_4, and g-C_3N_4(A) and photothermal conversion efficiency based on different materials(B)

photothermal effect. The optimal $Zn_xCo_3O_4$/g-C_3N_4 realizes the temperature from 20 °C to 66 °C. This great finding can effectively replace extra heating, which is very important in industry catalysis yield, especially for endothermic reactions.

3.2 Catalytic Performance Evaluation

To evaluate the catalytic performance of $M_xCo_3O_4$/g-C_3N_4, the epoxidation of styrene based on $M_xCo_3O_4$, g-C_3N_4 and $M_xCo_3O_4$/g-C_3N_4 has been investigated under visible light irradiation. The reactions ultilize acetonitrile as solvent, isobutyraldehyde as co-catalyst and O_2 molecular as oxidant. The chromatograms of reaction substates and target products corresponding to before and after the reaction, as well as the standard curves are identified by GC spectrometry (Figs.S2—S5, see the Electronic Supplementary Material of this paper).

As shown in Table 1, the activity of Co_3O_4 pyrolyzed by ZIF-67 is superior to that of commercial Co_3O_4, which can be ascribed to the exposed more active sites and easy substrate transfer through the mesoporous stucture(Entries 1 and 17, Table 1). Bimetallic $M_xCo_3O_4$(M=Zn, Ni, Fe) display higher activity and SO selectivity compared with monometallic oxide, Co_3O_4(Entries 2—4, Table 1), which is not hard to understand, because there are more active sites for bimetallic oxides. After assembly with g-C_3N_4, the composites exhibit enhanced catalytic activity taking advantage of the cooperative photothermal effects from both $M_xCo_3O_4$ and g-C_3N_4(Entries 10—12, Table 1). The endothermic property of styrene epoxidation has been demonstrated by the increased converson along with the rising reaction temperature(Figs.S6 and S7, see the Electronic Supplementary Material of this paper). It is worth noting that after Cu doping into Co_3O_4, the SO selectivity by $Cu_xCo_3O_4$ has been obviously enhanced when the Cu/Co molar ratio increases, and yet the conversion remains basically unchanged(Entries 5—8, Table 1). Similarly, after the recombination with g-C_3N_4, both conversion and selectivity for $Cu_xCo_3O_4$/g-C_3N_4 have been improved. Especially, the SO selectivity is even closed to 90%, exceeding those of most reported catalysts. To verify the oxygen source for styrene epoxidation, the reaction has been conducted under N_2 bubbling in the presence of isobutyraldehyde, in pure water without O_2 bubbling and isobutyraldehyde, or under O_2 bubbling without isobutyraldehyde, respectively, while no any products are detected(Entries 20—25, Table 1). The results illustrate the oxygen source is mainly from the bubbling O_2 molecule, yet the isobutyraldehyde as pro-oxygenic agent is indispensable. Herein, the probable epoxidation mechanism in the presence of sacrificial aldehydes is proposed, which is similar with previous

https://doi.org/10.1007/s40242-022-2292-6

reports[79,80]. The catalyst implements the free radical mechanism by adding O_2 and extracting [H] from aldehydes to form peroxy carboxylic acid(RCO_3H), and then promotes the transfer of [O] in RCO_3H to an alkene, finally producing the corresponding epoxide. Followed that, a hot filtration test is carried out for the mixture after 15 or 40 min, no any oxidized styrene is produced. The result indicates that the reaction process is truly heterogeneous(Fig.S8, see the Electronic Supplementary Material of this paper).

The catalytic activity comparison for the as-synthesized $M_xCo_3O_4$/g-C_3N_4 and previously reported catalysts toward styrene epoxidation reaction is summarized(Table S2, see the Electronic Supplementary Material of this paper). The data indicate that $Zn_xCo_3O_4$/g-C_3N_4 and $Cu_xCo_3O_4$/g-C_3N_4 give the best styrene conversion(>96%) and the highest SO selectivity(89%), respectively, compared with previous catalysts. Furthermore, the short reaction time and low temperature conditions make the catalysts more feasible in industry field.

In order to investigate the potential of catalysts in practical industry production, the recoverability and stability tests are explored. At the end of each cycle, the recovered catalyst is dried at 60 °C for 10 h, and then reused for next run under the same reaction conditions. As shown in Fig.6(A), the $Zn_xCo_3O_4$/g-C_3N_4 has almost unchanged catalytic activity even after 5 runs, revealing its excellent reusability and long life. For $Cu_xCo_3O_4$/g-C_3N_4, the slight decline of conversion and selectivity can be found. This is because a small quantity of Cu is oxided and then dissolved into reaction systerm in the presence of O_2[Fig.6(B)]. The changed solution color during the reaction process perfectly verifies above conjecture(Fig.S9, see the Electronic Supplementary Material of this paper). The corresponding ICP-AES analysis of the used $Cu_xCo_3O_4$/g-C_3N_4 also confirms a little leaching of Cu(Table S1).

The PXRD and TEM characterizations for $Zn_xCo_3O_4$/g-C_3N_4 and $Cu_xCo_3O_4$/g-C_3N_4 catalysts before and after recycles are shown in Fig.7. The unchanged diffraction peaks indicate the well retained crystal structure of MOF and good stability of $Zn_xCo_3O_4$/g-C_3N_4 in Fig.7(A). Furthermore, the size and regular morphology of $Zn_xCo_3O_4$/g-C_3N_4 after recycling test remain to be the same by TEM observation in Fig.7(B). These results demonstrate the excellent recycling stability of $Zn_xCo_3O_4$/g-C_3N_4.

Table 1 Reactions of photothermal styrene epoxidation[a]

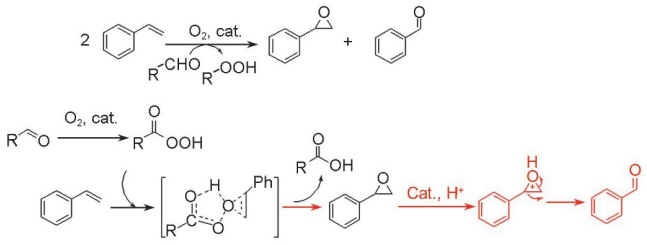

Entry	Precursor	Substrate	Con.(%)	Sel.(%) epoxide	Time/min
1	ZIF-67	Co_3O_4	92	57	50
2	Zn_1Co_2-ZIF	$Zn_xCo_3O_4$	96	78	20
3	Ni_1Co_2-ZIF	$Ni_xCo_3O_4$	95	67	20
4	Fe_1Co_2-ZIF	$Fe_xCo_3O_4$	92	75	40
5	Cu_1Co_2-ZIF	$Cu_xCo_3O_4$	91	67	50
6	Cu_1Co_1-ZIF	$Cu_xCo_3O_4$	79	67	50
7	Cu_2Co_1-ZIF	$Cu_xCo_3O_4$	95	74	50
8	Cu_5Co_1-ZIF	$Cu_xCo_3O_4$	91	75	50
9	ZIF-67/C_3N_4	Co_3O_4/C_3N_4	96	78	30
10	Zn_1Co_2-ZIF/g-C_3N_4	$Zn_xCo_3O_4$/g-C_3N_4	97	78	20
11	Ni_1Co_2-ZIF/g-C_3N_4	$Ni_xCo_3O_4$/g-C_3N_4	95	70	20
12	Fe_1Co_2-ZIF/g-C_3N_4	$Fe_xCo_3O_4$/g-C_3N_4	97	76	40
13	Cu_1Co_2-ZIF/g-C_3N_4	$Cu_xCo_3O_4$/g-C_3N_4	85	83	50
14	Cu_2Co_1-ZIF/g-C_3N_4	$Cu_xCo_3O_4$/g-C_3N_4	93	89	60
15[b,c]	Zn_1Co_2-ZIF/g-C_3N_4	$Zn_xCo_3O_4$/g-C_3N_4	—	—	60
16[b,c]	Cu_2Co_1-ZIF/g-C_3N_4	$Cu_xCo_3O_4$/g-C_3N_4	—	—	60
17[c]	—	Commercial Co_3O_4	11	50	60
18[c]	—	g-C_3N_4	—	—	60
19[c]	No catalyst	—	—	—	60
20[d]	Zn_1Co_2-ZIF/g-C_3N_4	$Zn_xCo_3O_4$/g-C_3N_4	—	—	60
21[d]	Cu_2Co_1-ZIF/g-C_3N_4	$Cu_xCo_3O_4$/g-C_3N_4	—	—	60
22[e]	Zn_1Co_2-ZIF/g-C_3N_4	$Zn_xCo_3O_4$/g-C_3N_4	—	—	60
23[e]	Cu_2Co_1-ZIF/g-C_3N_4	$Cu_xCo_3O_4$/g-C_3N_4	—	—	60
24[f]	Zn_1Co_2-ZIF/g-C_3N_4	$Zn_xCo_3O_4$/g-C_3N_4	—	—	60
25[f]	Cu_2Co_1-ZIF/g-C_3N_4	$Cu_xCo_3O_4$/g-C_3N_4	—	—	60

a. Reaction conditions: 0.1 mmol of styrene, 2 mmol of isobutyraldehyde, 20 mL of acetonitrile, 30 mg of catalyst, O_2 bubbling, visible light($\lambda \geqslant 420$ nm); *b*. the reaction was performed without visible light irradiation; *c*. no products, or negligible products; the reaction was performed under; *d*. N_2 atmosphere in the presence of isobutyraldehyde; *e*. water without O_2 bubbling and isobutyraldehyde; *f*. O_2 bubbling without isobutyraldehyde.

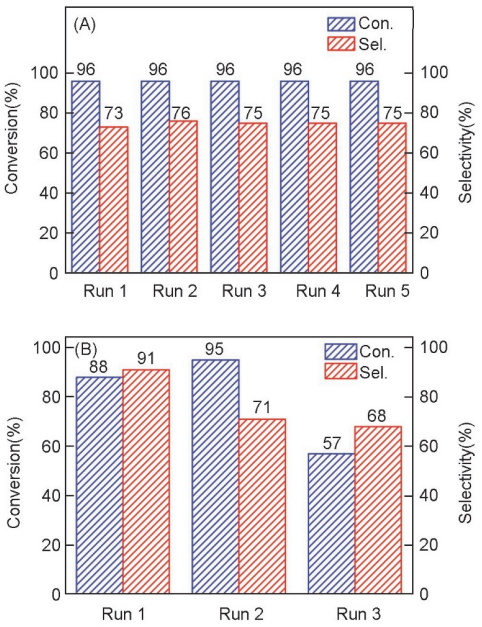

Fig.6 Recyclability test of five consecutive runs by $Zn_xCo_3O_4$/g-C_3N_4(A) and three consecutive runs by $Cu_xCo_3O_4$/g-C_3N_4(B)

https://doi.org/10.1007/s40242-022-2292-6

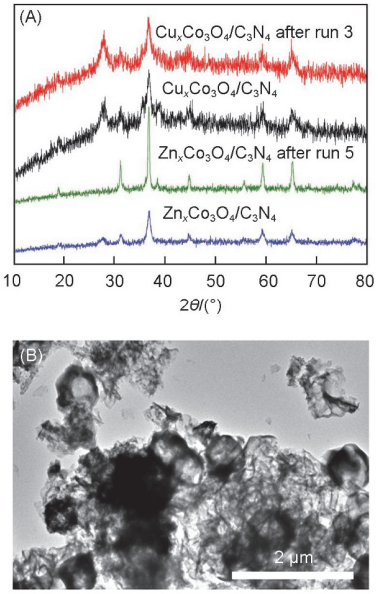

Fig.7 PXRD patterns of $Zn_xCo_3O_4$/g-C_3N_4 after 3 recycles and $Cu_xCo_3O_4$/g-C_3N_4 after 5 recycles(A) and TEM image of $Zn_xCo_3O_4$/g-C_3N_4 after catalytic cycles(B)

4 Conclusions

In summary, the composites consisted of bimetallic MCo-ZIFs and 2D g-C_3N_4 have been successfully calcinated to obtain $M_xCo_3O_4$/g-C_3N_4 catalysts at low temperature and air atmosphere. The hybrids achieve superhigh catalytic conversion of 96% or SO selectivity of 89% torward styrene epoxidation, compared with those of monometallic oxide and most reported catalysts. We attribute the outstanding catalytic performance to the the multiple active sites in $M_xCo_3O_4$ nanoparticles and the synthegistic photothermal effect from $M_xCo_3O_4$ and g-C_3N_4 under visible light, which greatly promotes the endothermic reaction. Recycling tests and corresponding characterizations results demonstate the good stability and recyclability of catalysts. This work represents the first research on the photothermal effect of ZIF-derived metal oxide. The finding might open a new opportunity to discover more novel functions of MOFs or explore more applications in various fields.

Electronic Supplementary Material

Supplementary material is available in the online version of this article at http://dx.doi.org/10.1007/s40242-022-2292-6.

Acknowledgements

This work was supported by the Excellent Youth Foundation of Shandong Natural Science Foundation, China(No.ZR2020YQ08), the National Natural Science Foundation of China(No.22275108) and the Key Research and Development Program of Shandong Province, China(No.2019GGX103043).

Conflicts of Interest

The authors declare no conflicts of interest.

References

[1] Tian S., Wang B., Gong W., He Z., Xu Q., Chen W., Zhang Q., Zhu Y., Yang J., Fu Q., Chen C., Bu Y., Gu L., Sun X., Zhao H., Wang D., Li Y., *Nat. Commun.*, **2021**, *12*, 1
[2] Punniyamurthy T., Velusamy S., Iqbal J., *Chem. Rev.*, **2005**, *105*, 2329
[3] Hu L., Yue B., Wang C., Chen X., He H., *Applied Catalysis A: General*, **2014**, *477*, 141
[4] Liu J., Meng R., Li J., Jian P., Wang L., Jian R., *Appl. Catal. B: Environ.*, **2019**, *254*, 214
[5] Liu Y, Tsunoyama H., Akita T., Tsukuda T., *Chem. Commun.*, **2010**, *46*, 550
[6] Choudhary V., Dumbre D., Patil N., Uphade B., Bhargava S., *J. Catal.*, **2013**, *300*, 217
[7] Zhang D., Li H., Li G., Chen J., *Dalton. Trans.*, **2009**, 10527
[8] Patil N., Uphade B., McCulloh D., Bhargava S., Choudhary V., *Catal. Commun.*, **2004**, *5*, 681
[9] Hu X., Bai J., Hong H., Li C., *Micropor. Mesopor. Mater.*, **2016**, *228*, 224
[10] Moon H., Limb A., Suh M., *Chem. Soc. Rev.*, **2013**, *42*, 673
[11] Zhou H., Kitagawab S., *Chem. Soc. Rev.*, **2014**, *43*, 5415
[12] Lee J., Farha O., Roberts J., Scheidt K., Hupp S., *Chem. Soc. Rev.*, **2009**, *38*, 1450
[13] Liu W., Huang J., Yang Q., Wang S., Sun X., Zhang W., Liu J., Huo F., *Angew. Chem. Int. Ed.*, **2017**, *56*, 5512
[14] Yu M., Space B., Franz D., Zhou W., He C., Li L., Krishna R., Chang Z., Li W., Hu T., Bu X., *J. Am. Chem. Soc.*, **2019**, *141*, 17703
[15] Bao S., Li J., Guan B., Jia M., Terasaki O., Yu J., *Matter*, **2020**, *3*, 498
[16] Wen Y., Rentería-Gómez Á., Day G., Smith M., Yan T., Ozdemir R., Gutierrez O., Sharma V., Ma X., Zhou H., *J. Am. Chem. Soc.*, **2022**, *144*, 11840
[17] Corma A., García H., Llabrés I., *Chem. Rev.*, **2010**, *110*, 4606
[18] Gao J., Huang Q., Wu Y., Lan Y., Chen B., *Adv. Energy. Sustain. Res.*, **2021**, *2*, 2100033
[19] Wang L., Li S., Chen Y., Jiang H., *Small*, **2021**, *17*, 2004481
[20] Sumida K., Rogow D., Mason J., McDonald T., Bloch E., Herm Z., Bae T., Long J., *Chem. Rev.*, **2012**, *112*, 724
[21] Lee Y., Moon H., Cheon Y., Suh M., *Angew. Chem. Int. Ed.*, **2008**, *47*, 7741
[22] Jaechul L., Chong Y., Jaheon K., Youngsuk K., Nakeun K., Seo Y., Kimoon K., Tae H., Lee E., *Angew. Chem. Int. Ed.*, **2018**, *57*, 7869
[23] Kim E., Siegelman R., Jiang H., Forse A., Lee J., Martell J., Milner P., Falkowski J., Neaton J., Reimer J., Weston S., Long J., *Science*, **2020**, *369*, 392
[24] Zhang Z., Wang H., Li Y., Xie M., Li C., Lu H., Peng Y., Shi Z., *Chem. Res. Chinese Universities*, **2022**, *38*(4), 750
[25] Li S., Gao Y., Li N., Ge L., Bu X., Feng P., *Energy Environ. Sci.*, **2021**, *14*, 1897
[26] Kaneti Y., Tang J., Salunkhe R., Jiang X., Yu A., Wu K., Yamauchi Y., *Adv. Mater.*, **2017**, *29*, 1604898
[27] Gu Z., Li D., Zheng C., Kang Y., Wöll C., Zhang J., *Angew. Chem. Int. Ed.*, **2017**, *56*, 6853
[28] Cao X., Tan C., Sindoro M., Zhang H., *Chem. Soc. Rev.*, **2017**, *46*, 2660
[29] Lide O., Tim W., Xiao H., Kapteijn F., Gascon J., *Mater. Chem. Front.*, **2017**, *1*, 1709
[30] Ma S., Goenaga G., Call A., Liu D., *Chem. Eur. J.*, **2011**, *17*, 2063
[31] Hu M., Reboul J., Furukawa S., Torad N., Ji Q., Srinivasu P., Ariga K., Kitagawa S., Yamauchi Y., *J. Am. Chem. Soc.*, **2012**, *134*, 2864
[32] Jiao L., Wan G., Zhang R., Zhou H., Yu S., Jiang H., *Angew. Chem. Int. Ed.*, **2018**, *57*, 8525
[33] Shah S., Najam T., Wen M., Zang S., Waseem A., Jiang H., *Small. Struct.*, **2022**, *3*, 2100090
[34] Jiao L., Zhang R., Wan G., Yang W., Wan X., Zhou H., Shui J., Yu S., Jiang H., *Nat. Commun.*, **2020**, *11*, 2831
[35] Srinivas G., Krungleviciute V., Guo Z., Yildirim T., *Energy Environ. Sci.*, **2014**, *7*, 335
[36] Kung C., Goswami S., Hod I., Wang T., Duan J., Farha O., Hupp J., *Acc. Chem. Res.*, **2020**, *53*, 1187
[37] Jiang H., Liu B., Lan Y., Kuratani K., Akita T., Shioyama H., Zong F., Xu Q., *J. Am. Chem. Soc.*, **2011**, *133*, *31*, 11854
[38] Zhang T., Lin W., *Chem. Soc. Rev.*, **2014**, *43*, 5982
[39] Liu B., Shioyama H., Akita T., Xu Q., *J. Am. Chem. Soc.*, **2008**, *130*, 5390
[40] Wang F., Li C., Chen H., Jiang R., Sun L., Li Q., Wang J., Yu J., Yan C., *J. Am. Chem. Soc.*, **2013**, *135*, 5588
[41] Song S., Wang X., Li S., Wang Z., Zhu Q., Zhang H., *Chem Sci.*, **2015**, *6*, 6420
[42] Zhang W., Wu Z., Jiang H., Yu S., *J. Am. Chem. Soc.*, **2014**, *136*, 14385
[43] Zhi G., Yu X., Zhao D., *Chem. Soc. Rev.*, **2021**, *50*, 4629
[44] Tang J., Salunkhe R., Liu J., Torad N., Imura M., Furukawa S., Yamauchi Y., *J. Am. Chem. Soc.*, **2015**, *137*, 1572

[45] Xiao C., Lin Y., Zhang J., Chen X., *Angew. Chem. Int. Ed.*, **2006**, *45*, 1557
[46] Li B., Liu J., Liu Q., Chen R., Zhang H., Yu J., Song D., Li J., Zhang M., Wang J., *Appl. Surf. Sci.*, **2019**, *475*, 700
[47] Chen Y., Wang C., Wu Z., Xiong Y., Xu Q., Yu S., Jiang H., *Adv. Mater.*, **2015**, *27*, 5010
[48] Zheng F., Yang Y., Chen Q., *Nat. Commun.*, **2014**, *5*, 5261
[49] Zhang S., Guan B., Lu X., Xi S., Du Y., Lou X., *Adv. Mater.*, **2020**, *32*, 2002235
[50] Rabani I., Zafar R., Subalakshmi K., Kim H., Bathula C., Seo Y., *J. Hazard. Mater.*, **2021**, *407*, 124360
[51] Su T., Lu G., Sun K., Zhang M., Cai C., *Catal. Sci. Technol.*, **2022**, *12*, 216
[52] Han Y., Li J., Zhang T., Qi P., Li S., Gao X., Zhou J., Feng X., Wang B., *Chem. Eur. J.*, **2018**, *24*, 1651
[53] Guo J., Wan Y., Zhu Y., Zhao M., Tang Z., *Nano. Res.*, **2021**, *14*, 2037
[54] Hao Y., Chen L., Li J., Guo Y., Su X., Shu M., Zhang Q., Gao W., Li S., Yu Z., Gu L., Feng X., Yin A., Si R., Zhang Y., Wang B., Yan C., *Nat. Commun.*, **2021**, *12*, 2682
[55] Jain P., Huang X., El-Sayed I., El-Sayed M., *Acc. Chem. Res.*, **2008**, *41*, 1578
[56] Yang Q., Xu Q., Yu S., Jiang H., *Angew. Chem. Int. Ed.*, **2016**, *55*, 3785
[57] Linic S., Aslam U., Boerigter C., Morabito M., *Nat. Mater.*, **2015**, *14*, 567
[58] Wang Y., Liu L., Ma T., Zhang Y., Huang H., *Adv. Funct. Mater.*, **2021**, *31*, 2102540
[59] Ismael M., *J. Alloy. Compd.*, **2020**, *846*, 156446
[60] Huang T., Fu Y., Peng Q., Yu C., Zhu J., Yu A., Wang X., *Appl. Surf. Sci.*, **2019**, *480*, 888
[61] Liu J., Wang H., Antonietti M., *Chem. Soc. Rev.*, **2016**, *45*, 2308
[62] Liu X., Yang W., Chen L., Liu Z., Long L., Wang S., Liu C., Dong S., Jia J., *ACS Appl. Mater. Inter.*, **2020**, *12*, 4463
[63] Bi L., Xu D., Zhang L., Lin Y., Wang D., Xie T., *Phys. Chem. Chem. Phys.*, **2015**, *17*, 29899
[64] Wang Y., Wang X., Antonietti M., *Angew. Chem. Int. Ed.*, **2012**, *51*, 68
[65] Yang L., Liu J., Yang L., Zhang M., Zhu H., Wang F., Yin J., *Renew. Energ.*, **2020**, *145*, 691
[66] Liu D., Chen D., Li N., Xu Q., Li H., He J., Lu J., *Small*, **2019**, *15*, 1902291
[67] Gu W., Hu L., Li J., Wang E., *ACS. Appl. Mater. Inter.*, **2016**, *8*, 35281
[68] Wang R., Yan T., Han L., Chen G., Li H., Zhang J., Shi L., Zhang D., *J. Mater. Chem. A*, **2013**, *6*, 5752
[69] Zhu Z., Chen C., Wu R., *J. Chin. Chem. Soc.*, **2020**, *67*, 1654
[70] Luo D., Liu S., Liu J., Zhao J., Miao C., Ren J., *Ind. Eng. Chem. Res.*, **2018**, *57*, 11920
[71] Muniandy L., Adam F., Mohamed A., Iqbal A., Rahman N., *Appl. Surf. Sci.*, **2017**, *398*, 43
[72] Cao S., Low J., Yu J., Jaroniec M., *Adv. Mater.*, **2015**, *27*, 2150
[73] Zhou Q., Zhang Z., Cai J., Liu B., Zhang Y., Gong X., Sui X., Yu A., Zhao L., Wang Z., Chen Z., *Nano Energy*, **2020**, *71*, 104592
[74] Banerjee R., Phan A., Wang B., Knobler C., Furukawa H., O'Keeffe M., Yaghi O., *Science*, **2008**, *319*, 939
[75] Wang P., Zhang X., Shi R., Zhao J., Yuan Z., Zhang T., *Energy Fuels*, **2022**, *36*, 11627
[76] Chen H., Shi R., Zhang T., *Molecules*, **2021**, *26*, 7552
[77] Li Y., Li R., Li. Z, Xu Y., Yuan H., Ouyang S., Zhang T., *Solar RRL*, **2022**, *6*, 2200493
[78] Wang Y., Wu X., Shao B., Yang X., Owens G., Xu H., *Sci. Bull.*, **2020**, *65*, 1380
[79] Bastienne B., Patricia A., Feiters M., Nolte R., *J. Chem. Soc., Dalton Trans.*, **1998**, 2241
[80] Gansäuer A., Lauterbach T., Narayan S., *Angew. Chem. Int. Ed.*, **2003**, *42*, 5556